Supplementary material for:

A thermal energy storage composite with sensing function and its thermal conductivity and thermal effusivity enhancement

Hong Lei,*[a] Chunfang Fu,[a] Yajun Zou, [a] Shiyan Guo [a] and Jichuan Huo *[a]

[a] State Key Laboratory of Environment-friendly Energy Materials, School of Materials Science and Engineering, Southwest University of Science and Technology, Mianyang 621010, People's Republic of China

* Corresponding author. Tel: + 86 816 2419201. Fax: + 86 816 2419201. E-mail: honglei117@163.com (H. Lei); huojichuan@swust.edu.cn (J. Huo).

Supplementary Figures:

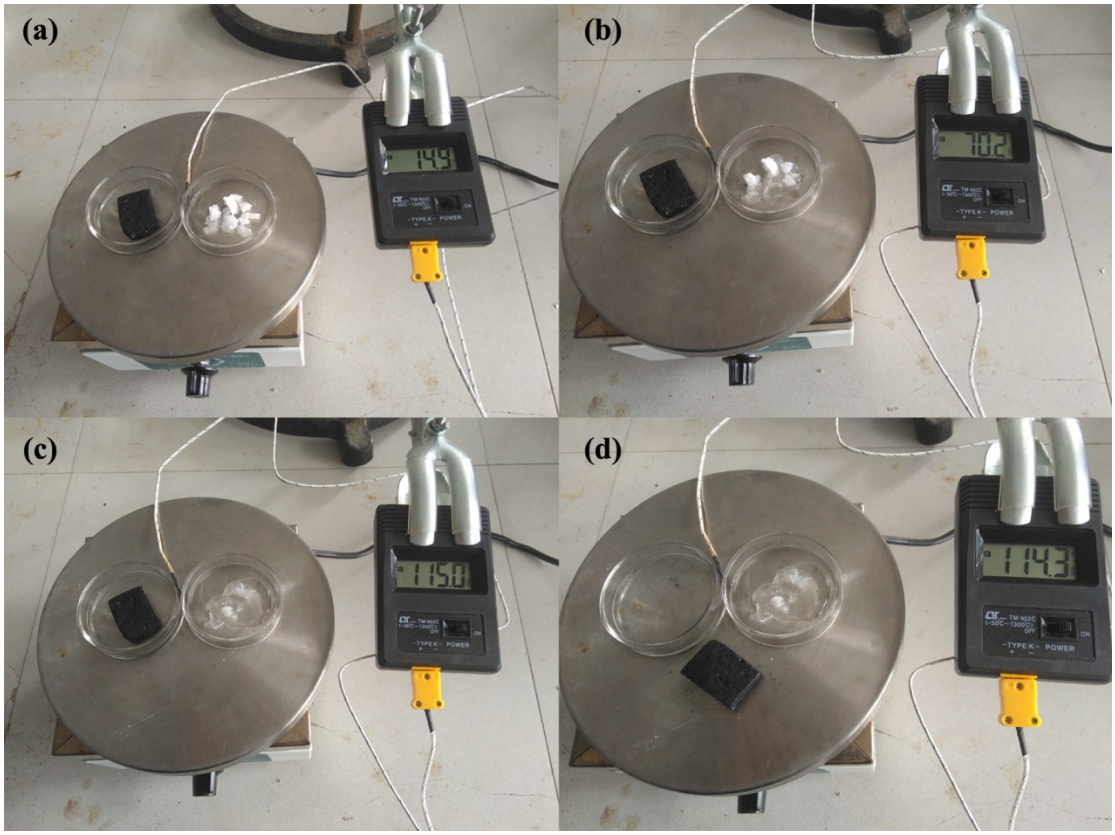

Figure S1. Appearance comparison of CF-PPy-PCM-24-5 and mixture of PEG-1000, PEG-2000 and $CaCl_2 \cdot 6H_2O$ at different temperatures: no leakage of CF-PPy-PCM-24-5 was observed during heating and cooling.

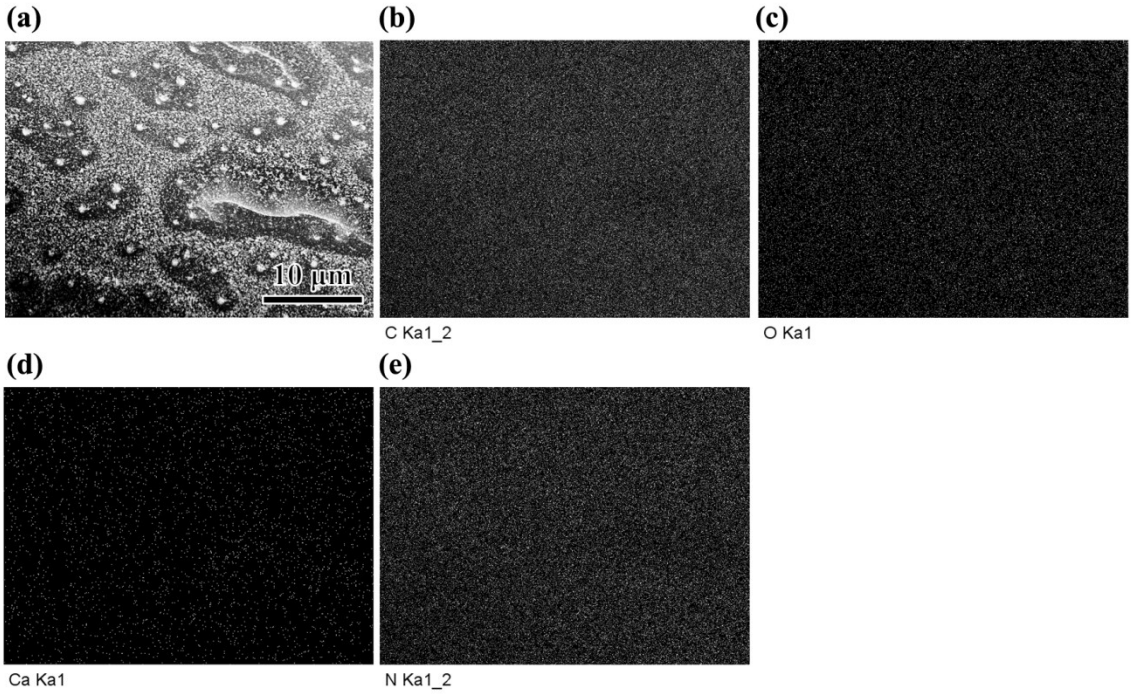

Figure S2. (a) SEM image and (b-e) the corresponding EDX Mapping images of CF-PPy-PCM-24-15

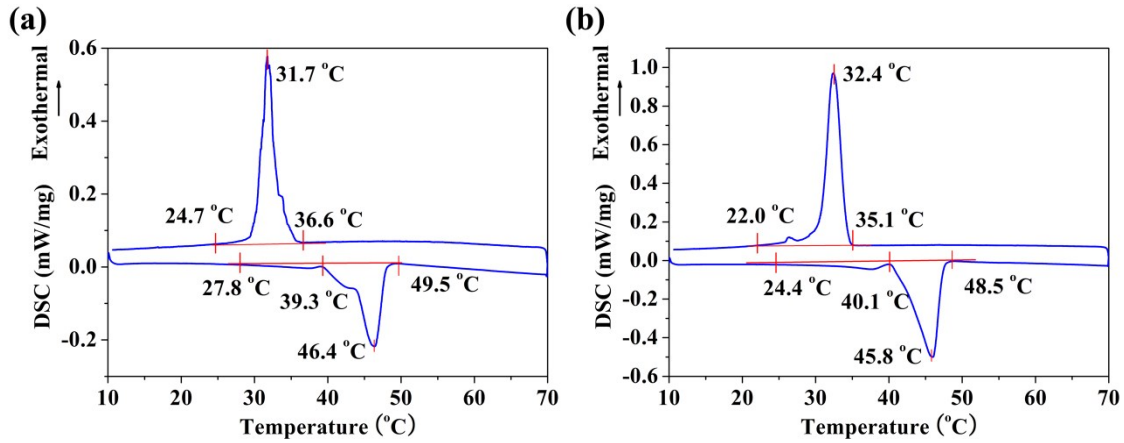

Figure S3. The DSC curves of (a) CF-PPy-PCM-24-15 and (b) CF-PPy-PCM-24-5

Supplementary Tables:

Table S1. Densities and thermophysical properties of CF, CF-PPy-24, CF-PPy-PCM-24-15 and CF-PPy-PCM-24-5.

Sample	CF	CF-PPy-24	CF-PPy-PCM-24-15	CF-PPy-PCM-24-5
ρ/kg m^{-3}	153	165	383	634
ΔH_m (J g^{-1})	/	/	24.47	54.66
ΔT (K)	/	/	21.7	24.1
$\overline{C_p}$ /J kg^{-1} K^{-1}	750[a)]	840[a)]	1128	2268
α/mm^2 s^{-1} (//)[c)]	24.2	61.0	68.6	68.2
α/mm^2 s^{-1} ($\perp$) [c)]	18.2	81.0	88.7	87.9
k/W m^{-1} K^{-1} (//)	2.8[b)]	8.5[b)]	29.6	98.1
k/W m^{-1} K^{-1} ($\perp$)	2.1[b)]	11.2[b)]	38.3	126.4
e/kJ m^{-2} K^{-1} s$^{-1/2}$ (//)	0.6[b)]	1.1[b)]	3.6	11.9
e/kJ m^{-2} K^{-1} s$^{-1/2}$ ($\perp$)	0.5[b)]	1.2[b)]	4.1	13.5

[a)] Estimated according to literature [1]; [b)] Calculated based on the estimated values; [c)] Measured at 65 °C.

Table S2. Data used to construct the plot of thermal conductivity (*k*) and thermal effusivity (*e*) in literature and this work.

Sample	*k*/W m^{-1} K^{-1}	*e*/kJ m^{-2} K^{-1} $s^{-1/2}$
Ref. [2]	3.5	9.0
Ref. [2]	10.4	15.5
Ref. [3]	2.8	2.3
Ref. [3]	2.7	2.3
Ref. [3]	2.6	2.3
Ref. [3]	1.9	2.6
Ref. [3]	1.9	2.7
Ref. [3]	1.8	2.7
Ref. [4]	1.2	1.3
Ref. [5]	20	5.5
Ref. [6]	13	6.80
Ref. [6]	5	4.12
Ref. [7]	20.2	6.32
Ref. [7]	20.2	6.64
Ref. [8]	16.6	5.09
Ref. [9]	23.3	17.13
Ref. [10]	7.32	8.85
CF-PPy-PCM-24-15	29.6(//), 38.3(⊥)	3.6(//), 4.1(⊥)
CF-PPy-PCM-24-5	98.1(//), 126.4(⊥)	11.9(//), 13.5(⊥)

Supplementary Note 1:

Supplementary explanation for the values of thermal effusivity in **Table S2**.

It should be noted that some of the *e* values in **Table S2** are directly provided by the references, while some others are calculated based on the relevant parameters reported therein. If the data in the references is presented in an image format, the data is obtained from the relative positions of the pixels in the coordinate system. Details are as follows.

- Ref. [2]: According to Cottrill et al, if a phase change material (PCM) is utilized in a dynamic environment in proximity to its phase transition temperature, C_p should be replaced by the latent heat per unit mass of the PCM during the calculation of effective thermal effusivity. But this will result in a unit difference of $K^{-1/2}$ between the obtained thermal effusivity and those reported in many other literatures. For ease of comparison, the unit of e_{ff} was converted according to Equation (S1) and the DSC curve in the supplementary materials of Ref. [2]. The *e* values of Ref. [2] in **Table S2** were obtained by dividing the original e_{ff} values in Ref. [2] by $\sqrt{\Delta T}$ (Equation (S2)).
- Ref. [3]: The *e* values were calculated by Equation (S3) using the thermal diffusivity, density and specific heat capacity provided by Ref. [3].
- Ref. [4]: The *e* value was directly provided by Ref. [4].
- Ref. [5]: The *e* value was read from the Figures of Ref. [5].
- Ref. [6], Ref. [9] and Ref. [10]: Firstly, the values of ΔT were obtained from the DSC curves. The values of C_p were then calculated using Equation (S1) based on

the latent heat data provided by the literatures. Finally, the values of *e* were obtained according to Equation (S4).

- Ref. [7] and Ref. [8]: The values of *e* were calculated using Equation (S4) based on the thermal conductivity, density and specific heat capacity provided by the literatures.

The equations used in the calculation are as follows:

$$\overline{C_p} = \frac{\Delta H_m}{\Delta T} = \frac{\Delta H_m}{T_{end} - T_{onset}} \tag{S1}$$

$$e = \sqrt{k \cdot \rho \cdot \Delta H_m} / \sqrt{\Delta T} = e_{eff} / \sqrt{\Delta T} \tag{S2}$$

$$e = \sqrt{\alpha} \rho C_p \tag{S3}$$

$$e = \sqrt{k \cdot \rho \cdot C_p} \tag{S4}$$

$\overline{C_p}$ or C_p: average specific heat capacity or specific heat capacity;

ΔH_m: latent heat per unit mass of the PCM;

ΔT: temperature interval of phase change;

T_{end}: the temperature at which the PCM is completely melted;

T_{onset}: the temperature at which the PCM begins to melt;

e: thermal effusivity;

e_{eff}: effective thermal effusivity in Ref. [2];

k: thermal conductivity;

ρ: density of TES composite;

α: thermal diffusivity.

Supplementary Note 2:

The derivation process of the modified parallel model.

As shown in **Figure 6b**, if we assume that the part 1 represents a highly thermally conductive skeleton, the part 2 represents PCMs, and the part 3 represents air, the effective thermal conductivity (k_{eff}) of the composite should be depicted as Equation (S5) according to the parallel model. The k_1, k_2 and k_3 represent the thermal conductivities of part 1, 2 and 3, while the v_1, v_2 and v_3 are the volume fractions of the three parts, respectively.

$$k_{eff} = v_1 \cdot k_1 + v_2 \cdot k_2 + v_3 \cdot k_3 \tag{S5}$$

However, if the heat conduction from part 1 to part 2 and the heat storage of part 2 are considered, the total heat flux flowing into the composite (dQ/dt) will consist of four items according to the conservation of energy. Namely, in addition to the heat flux through the part 1, 2 and 3 (i.e., dQ_1/dt, dQ_2/dt and dQ_3/dt), the heat flux conducted from the part 1 to the part 2 (dQ_{12}/dt) should also be considered. Then the parallel model should be modified as follows.

$$\frac{dQ}{dt} = \frac{dQ_1}{dt} + \frac{dQ_2}{dt} + \frac{dQ_3}{dt} + \frac{dQ_{12}}{dt} \tag{S6}$$

$$-k_{eff} \cdot \frac{\partial T}{\partial y} \cdot A = -k_1 \cdot \frac{\partial T}{\partial y} \cdot A_1 - k_2 \cdot \frac{\partial T}{\partial y} \cdot A_2 - k_3 \cdot \frac{\partial T}{\partial y} \cdot A_3 + \rho_{PCM} \cdot L_{PCM} \cdot v_x \cdot A_{12} \tag{S7}$$

Dividing both sides simultaneously by $(-\frac{\partial T}{\partial y} \cdot A)$ yields Equation (S8).

$$k_{eff} = v_1 \cdot k_1 + v_2 \cdot k_2 + v_3 \cdot k_3 - \rho_{PCM} \cdot L_{PCM} \cdot v_x \cdot \frac{A_{12}}{A} \cdot \frac{1}{\partial T / \partial y} \tag{S8}$$

In the above equations, A, A_1, A_2 and A_3 are the areas of the heat flow path through

the composite, part 1, 2, and 3, respectively. A_{12} is the area of the heat flow path between part 1 and 2. ρ_{PCM} and L_{PCM} represent the density and latent heat of the PCMs (i.e., part 2), respectively. v_x is the velocity of the solid-liquid interface in part 2. In the vicinity of the phase change temperature of the part 2, we have the relationship shown in Equation (S9), where the effective thermal conductivity (k_{eff}) is equal to the product of the thermal diffusivity ($\alpha_{composite}$), density ($\rho_{composite}$) and average effective specific heat capacity ($\overline{C_{p,eff}}$) of the composite. If we bring Equation (S9) into Equation (S8), we will get Equation (S10).

$$k_{eff} = \alpha_{composite} \cdot \rho_{composite} \cdot \overline{C_{p,eff}} \tag{S9}$$

$$\overline{C_{p,eff}} = \frac{v_1 \cdot k_1 + v_2 \cdot k_2 + v_3 \cdot k_3}{\rho_{composite} \cdot \alpha_{composite}} - \frac{\rho_{PCM} \cdot L_{PCM} \cdot v_x \cdot \frac{A_{12}}{A} \cdot \frac{1}{\partial T / \partial y}}{\rho_{composite} \cdot \alpha_{composite}} \tag{S10}$$

On the other hand, the $\overline{C_{p,eff}}$ can also be depicted by Equation (S11) and further by Equation (S12) according to its definition.

$$\overline{C_{p,eff}} = \frac{dQ}{m_{composite} \cdot dT} = \frac{dQ_1 + dQ_2 + dQ_3}{m_{composite} \cdot dT} + \frac{dQ_{12}}{m_{composite} \cdot dT} \tag{S11}$$

$$\overline{C_{p,eff}} = \frac{dQ_1 + dQ_2 + dQ_3}{m_{composite} \cdot dT} + \frac{\rho_{PCM} \cdot L_{PCM} \cdot v_x \cdot A_{12}}{m_{composite} \cdot \frac{\partial T}{\partial t}} \tag{S12}$$

Comparing Equation (S10) and Equation (S12), we get Equation (S13). Then the Equation (S10) can be written as Equation (S14), and the k_{eff} and effective thermal effusivity (e_{eff}) of the composite can be described by Equation (S15) and Equation (S16).

$$-\frac{\rho_{PCM}\cdot L_{PCM}\cdot v_x\cdot \frac{A_{12}}{A}\cdot\frac{1}{\partial T/\partial y}}{\rho_{composite}\cdot\alpha_{composite}}=\frac{\rho_{PCM}\cdot L_{PCM}\cdot v_x\cdot A_{12}}{m_{composite}\cdot\frac{\partial T}{\partial t}} \quad \text{(S13)}$$

$$\overline{C_{p,eff}}=\frac{v_1\cdot k_1+v_2\cdot k_2+v_3\cdot k_3}{\rho_{composite}\cdot\alpha_{composite}}+\frac{\rho_{PCM}\cdot L_{PCM}\cdot v_x\cdot A_{12}}{m_{composite}\cdot\frac{\partial T}{\partial t}} \quad \text{(S14)}$$

$$k_{eff}=\alpha_{composite}\cdot\rho_{composite}\cdot\overline{C_{p,eff}} \quad \text{(S15)}$$

$$e_{eff}=\sqrt{k_{eff}\cdot\rho_{composite}\cdot\overline{C_{p,eff}}}=\sqrt{\alpha_{composite}}\cdot\rho_{composite}\cdot\overline{C_{p,eff}} \quad \text{(S16)}$$

Actually, the A_{12} may be much larger than the contact area between the composite and the heat source (A). Considering the contribution of the latent heat of PCMs (L_{PCM}) to the fourth term in Equation (S14) and the dQ_{12}/dt in the Equation (S6) may be much larger than the sum of dQ_1/dt, dQ_2/dt and dQ_3/dt, the k_{eff} of the composite may become much larger than that before the introduction of PCMs (i.e., $v_1\cdot k_1+(v_2+v_3)\cdot k_3$) if the thermal diffusivity of the composite ($\alpha_{composite}$) does not change much. Generally, the PCMs contribute much more to the specific heat capacity of the TES-composite than its matrix. Then the $\overline{C_{p,eff}}$, k_{eff} and e_{eff} may be simply expressed as follows.

$$\overline{C_{p,eff}}=\frac{\rho_{PCM}\cdot L_{PCM}\cdot v_x\cdot A_{12}}{m_{composite}\cdot\frac{\partial T}{\partial t}} \quad \text{(S17)}$$

$$k_{eff}=\alpha_{composite}\cdot\rho_{composite}\cdot\frac{\rho_{PCM}\cdot L_{PCM}\cdot v_x\cdot A_{12}}{m_{composite}\cdot\frac{\partial T}{\partial t}} \quad \text{(S18)}$$

$$e_{eff}=\sqrt{\alpha_{composite}}\cdot\rho_{composite}\cdot\frac{\rho_{PCM}\cdot L_{PCM}\cdot v_x\cdot A_{12}}{m_{composite}\cdot\frac{\partial T}{\partial t}} \quad \text{(S19)}$$

References

[1] Uddin K., Islam M. A., Mitra S., Lee J., Thu K., Saha B. B., Koyama S., Specific heat capacities of carbon-based adsorbents for adsorption heat pump application. Appl. Therm. Eng., 2018, 129: 117-126.

[2] Cottrill A. L., Liu A. T., Kunai Y., Koman V. B., Kaplan A., Mahajan S. G., Liu P., Toland A. R., Strano M. S., Ultra-high thermal effusivity materials for resonant ambient thermal energy harvesting. Nat. Commun., 2018, 9: 664-674.

[3] Karthik M., Faik A., D'Aguanno B., Graphite foam as interpenetrating matrices for phase change paraffin wax: A candidate composite for low temperature thermal energy storage. Sol. Energ. Mat. Sol. C., 2017, 172: 324-334.

[4] Xiao X., Zhang P., Morphologies and thermal characterization of paraffin/carbon foam composite phase change material. Sol. Energ. Mat. Sol. C., 2013, 117: 451-461.

[5] Acem Z., Lopez J., Del Barrio E. P., $KNO_3/NaNO_3$ - Graphite materials for thermal energy storage at high temperature: PartI. - Elaboration methods and thermal properties. Appl. Therm. Eng., 2010, 30: 1580-1585.

[6] Huang Z., Gao X., Xu T., Fang Y., Zhang Z., Thermal property measurement and heat storage analysis of $LiNO_3$/KCl - expanded graphite composite phase change material. Appl. Energ., 2014, 115: 265-271.

[7] Mallow A., Abdelaziz O., Graham Jr. S., Thermal charging study of compressed expanded natural graphite/phase change material composites. Carbon, 2016, 109: 495-504.

[8] Mills A., Farid M., Selman J. R., Al-Hallaj S., Thermal conductivity enhancement

of phase change materials using a graphite matrix. App. Therm. Eng., 2006, 26: 1652-1661.

[9] Wu S., Li T. X., Yan T., Dai Y. J., Wang R. Z., High performance form-stable expanded graphite/stearic acid composite phase change material for modular thermal energy storage. Int. J. Heat Mass Tran., 2016, 102: 733-744.

[10] Xu T., Chen Q., Huang G., Zhang Z., Gao X., Lu S., Preparation and thermal energy storage properties of D-Mannitol/expanded graphite composite phase change material. Sol. Energ. Mat. Sol. C., 2016, 155: 141-146.